The Nature of Infill Material on the Discontinuities of the Muntele Mare Granite (Beliş-Fantânele, Romania)

Nicolae Har (nicolae.har@ubbcluj.ro)
Babes-Bolyai University: Universitatea Babes-Bolyai https://orcid.org/0000-0002-7332-8969
Robert Gheorghiu
Babes-Bolyai University: Universitatea Babes-Bolyai

Research Article

Keywords: granite, secondary phases, discontinuities, infill material, slope stability

Posted Date: March 30th, 2021

DOI: https://doi.org/10.21203/rs.3.rs-344600/v1

THE NATURE OF INFILL MATERIAL ON THE DISCONTINUITIES OF THE MUNTELE MARE GRANITE (BELIŞ-FANTÂNELE, ROMANIA)

Nicolae HAR[a, 1], Robert Ionel GHEORGIU[a]

[a] Department of Geology, Babes-Bolyai University Cluj Napoca, 1 Kogălniceanu Str., 400084, Romania

Abstract:

The stability of rock massifs is strongly influenced by natural degradation processes. In combination with hydrothermal activity or atmospheric exposure, rock alteration processes can lead to the formation of secondary phases that ultimately control the rock quality and slope stability, which are particularly important for engineering works (e.g., road cuts, open pits, quarries, tunnels). The Bozgai open quarry in the Muntele Mare granite massif in the northern Apuseni Mountains (Romania) offers an excellent opportunity to investigate the influence of alteration processes on rock properties, especially owing to the extensive exposure of granite and specific mineral assemblages of hydrothermal genesis to atmospheric conditions. The alteration processes generated secondary phases located on the primary minerals of the affected rocks or deposited as infill material along the granite discontinuities. Natural and oriented samples of the Bozgai quarry infill material were investigated using polarized light, X-ray diffraction, and scanning electron microscopy to obtain images and identify their mineralogical composition. The hydrothermal vein material consists of kaolinite, illite, pyrite, marcasite, quartz, iron hydroxides, albite, and microcline. These samples were exposed to atmospheric oxygen and meteoric water and secondary sulphates (jarosite and gypsum) formed in an acidic environment generated by the oxidization of pyrite and marcasite. The sheeted structure of kaolinite and geochemical behavior of the sulphates in the presence of water play a particularly important role in the reduced rock slope stability in the Bozgai quarry.

Key words: granite, secondary phases, discontinuities, infill material, slope stability

[1] Corresponding author. Department of Geology, Babeş Bolyai University, 1 Kogălniceanu Str., Cluj Napoca, România. E-mail: nicolae.har@ubbcluj.ro

I. Introduction

The Muntele Mare granite massif consists of a main batholite and two small related magmatic bodies and is located in the central and northern part of the Apuseni Mountains (Romania) between Arieş Valley to the south and Beliş area in the north. Granitic rocks are extensively exposed in this area along natural outcrops, cut road slopes, and in the Bozgai quarry in Beliş where material was extracted in the 1970s to construct the Beliş-Fântânel Dam. These locations provide ample opportunity to investigate the primary mineralogy, secondary alteration products that developed on the primary minerals, and associated discontinuities (Fig. 1). The granitic magmatic bodies recorded important sets of discontinuities resulting from a brittle alpine tectonic event, and infill material is present on the discontinuities in some cases.

Advanced rock slope instability has been detected in the upper part of the Bozgai quarry owing to rock weathering from exposure to meteoric water. Rock slope stability and the quality of extracted aggregates are largely influenced by weathering processes, in addition to the spatial distribution of joints and faults, orientation, persistence, and spacing. Hydrothermal and supergene rock alteration in the presence of meteoric water and atmospheric oxygen can lead to the formation of infill material on the discontinuities, which also exerts an important control over rock slope stability (Wyllie and Mah 2004).

The granitic rock form Muntele Mare massif has been the subject of several scientific papers focused mainly on its geology, petrography, geochemistry and tectonic setting (Dumitrescu, 1966; Săndulescu, 1984; Pană, 1998; Anton, 1999; Balintoni, 2009). None of these studies dealt with the alteration processes of the granitic rocks.

Many studies that address the problem of alteration of granitic rocks are known in the literature. Most of them deal with the alteration of rock-forming primary minerals and resulted saprolite with specific clay minerals assemblages, usually developed on the top of the granitic body (Meunier and Velde, 1982; Braga et al., 2002; Kirschbaum et al., 2005; Oberhardt, 2013). The alteration took place under the influence of several factors as parental material, time, climate, topography and living organism (Hill, 1995; Wilson, 2004). Bustin & Matthews (1979) in the study of the processes of alteration of the granitic clasts transported by glacier suggests the possibility of hydrothermal alteration of the rock prior to glacial transport account for the variable degree of disintegration at their present sites. Lee et al, (2007) identified the acide rains as an important factor affecting the granitic rocks with characteristic changes in chemical composition and mineralogy.

The formation of local acidic environment as the result of iron sulfides decomposition were described by Cravotta (1994) and Hammarstrom et al., (2001) during weathering processes of mining waste and tailing piles with metal-sulfides content or in the alteration processes of sulfide containing aggregates from asphat mixture (Har et. al, 2019). Pyrite and marcasite of hydrothermal genesis were identified in the studied area and their alteration generated local acidic environment responsible for some degradation processes of Muntele Mare granite defined by typical secondary mineral phases.

In this study, seven benches of the Bozgai open quarry in the northern part of the Muntele Mare massif were investigated to identify the factors that contribute to the degradation of the granitic rock. Infill material on the discontinuities is mainly present in the upper part of the quarry in a debris cone of weathered magmatic rock (Fig. 2). The most intense weathered rocks are located specifically at the contact between the granitic host rock and an andesitic intrusion. A spatial relationship is evident between the hydrothermal alteration generated by the andesitic intrusion and distribution of the secondary mineral assemblages developed as infill material in the granitic rock discontinuities. The aims of the present study are to identify the weathering processes that affect the magmatic rocks of the Bozgai quarry, determine the nature of the infill material on the discontinuities, and assess the influence of these phenomena on the pit slope stability.

II. Methods of study

Different analytical methods were used to investigate the degradation processes affecting the Bozgai quarry rocks and corresponding secondary mineral phases. In situ macroscopic observations were used to select the most representative samples. A Nikon stereomicroscope was used to investigate the weathered rock samples. Binocular observations were used to select rock samples for thin section preparation and weathered products were selected and gold coated for further investigation using a scanning electron microscope (SEM). Thin sections were analyzed using a polarized-light Nikon Optiphot T2-Pol microscope and images were collected. X-ray diffraction (XRD) was performed on natural and oriented specimens to identify the secondary mineral phases using a Bruker D8 Advance diffractometer with Cu Kα radiation (λ = 1.541874 Å), a 0.01-mm Fe filter, and a LynxEye one-dimensional detector in the Department of Geology, Babeș-Bolyai University (Cluj-Napoca, Romania). Oriented aggregate mounts were prepared for XRD analysis following the typical procedure for clay minerals. The silt and clay-sized fractions were extracted from the first 5 cm of the suspension after decantation. The suspension was left for 1 h at 20 °C prior to extraction. The resulting clay and silt suspension was centrifuged at 3500 rpm for 10 min. The sediment that collected on the bottom of the

centrifuge tube was used to mount the oriented clay mineral samples. A thin film of concentrated suspension from each sample was spread over a glass slide and dried.

The working XRD parameters were 40 kV and 40 mA. Data were collected between 5° and 64° 2Θ with a step interval of 0.02° 2Θ and counting time of 0.2 s/step. The mineral phases were identified using the PDF2 database.

A JEOL JSM 5510 LV SEM with an Oxford Instruments INCA 300 energy dispersion X-ray spectrometer (EDS) was used to (semi)quantitatively determine the chemical composition of the mineralogical phases. The EDS was calibrated every 2 h using Oxford Instruments test specimens.

III. Geological data

The Variscan granitic massif of Muntele Mare in the North Apuseni Mountains (290.9±3.0 Ma; Balintoni et al. 2009) occurs as a main batholite of granitic composition accompanied by small isolated bodies (Fig. 3). The magmatic bodies are located in the metamorphic Someş Lithogroup and together represent the Bihor Autochthonous of the Apuseni Mountains.

Four main granite varieties were identified by Anton (1999) in the constitution of the Muntele Mare granite massif: biotite granodiorite; porphyritic biotite-muscovite granite; leucogranite; and equigranular muscovite-biotite granite. Andesitic sills and dykes of Upper Cretaceous age (Ştefan et al. 1988) up to 5–8 m in thickness intruded the schistosity planes of the surrounding metamorphic rocks on the contact limit between the granitic and metamorphic rocks, as well as on some tectonic discontinuities in the main granitic body. Hydrothermal activity followed by supergene alteration led to the formation of some secondary minerals as infill material on the discontinuities.

Two types of parental rocks are present in the study area: equigranular muscovite-biotite granite and porphyritic andesite. The granite is pierced by a porphyritic andesite dyke, which is highly visible from the 2nd to 6th quarry benches and gradually decreases in thickness from approximately 8 m in the lower part to 2–2.5 m in the upper part.

III.1. Petrography of parental rocks

Granite. Equigranular muscovite-biotite microgranite (Plate I, a) with a holocrystalline-massive texture is the main rock extracted in the Bozgai quarry and porphyritic biotite-muscovite granite is also locally present (Plate I, b). These rocks consist of quartz, orthoclase, microcline, plagioclase feldspars, muscovite, and biotite as the main components (Plate I, a and b) and zircon and apatite as accessory

minerals. K-feldspars are present as porphyritic phenocrysts. Tourmaline and opaque minerals are also present as individual crystals or granular masses as the infill of small veins (<1-mm thick).

The granitic rocks at the contact with the andesitic dyke were affected by hydrothermal solutions released by the andesite (Fig. 2). There is a gradual/zoned distribution of secondary products in the granitic rock as the result of gradual weathering intensity as follows.

- Highly intense alteration of feldspars near the andesite-granite contact. Both K- and plagioclase feldspars are entirely replaced by secondary minerals; namely, clay minerals and sericite (Plate I, c - d). The presence of rusty-colored iron hydroxides as secondary products indicates the former presence of mafic minerals (e.g., biotite) or iron sulfides and is associated with fresh minerals including quartz and muscovite.
- A lower alteration degree in the external contact zone area, with feldspars partly transformed into clay minerals and sericite (Plate I, e-f). The primary crystals remain preserved and the secondary products are uniform distributed on the primary mineral surface or as nestlings of fine crystals.

Porphyritic andesite. These samples are black to green in color with a very fine grain size typical of volcanic rocks. Under the microscope, the samples show a porphyritic texture with very fine groundmass and were strongly affected by hydrothermal alteration (Plate II, a–d).

Both the phenocrysts and crystals of the groundmass are entirely replaced by secondary minerals. Two secondary paragenesis features developed on the primary minerals:

- Sericite, clay minerals, and calcite, which indicate the former presence of plagioclase feldspars (Plate II, a–c);
- Chlorite, sericite, and opaque minerals, which indicate the former presence of biotite (Plate II, b and c);

Small polysynthetic twinned plagioclase crystals in the groundmass are still visible under the microscope (Plate II, c) associated with sericite, clay minerals, chlorite, calcite, and opaque minerals, and contain small veins infilled with quartz and metallic minerals (Plate II, c) or iron hydroxides (Plate II, d).

III.2. Rock alteration and infill material

Typical minerals precipitated as the infill material of the small veins that cross both the andesitic and granitic rocks owing to the andesite-related hydrothermal activity. Secondary minerals formed on the feldspars and mafic minerals (e.g., biotite) of both rock types in the presence of hydrothermal solutions. The XRD investigation of the material collected from such hydrothermal veins (sample 790)

shows an assemblage consisting of quartz, calcite, pyrite, marcasite, illite, kaolinite, and muscovite/sericite (Fig. 4, Table 1).

The iron sulfides (e.g., pyrite and marcasite) degraded under atmospheric conditions in the presence of water, oxygen, and CO_2. Friable white- to yellowish-colored secondary products precipitated in the granite weathering zone in the proximity of the andesitic dyke. Some are rusty in color owing to the presence of iron hydroxides or other iron-bearing secondary minerals and developed as thin crusts (<1-mm thick), fine granular masses on the surface of the granitic fragments, or as infill material on the rock discontinuities (Fig. 5).

Four samples of the infill material (794-6, 794-7, 795-2, and 796-1) were collected for detailed mineralogical investigations based on the macroscopic features (color, crystal size, spatial relationship with the host rock). The XRD results (Fig. 6) indicate that the mineralogic assemblages are dominated by quartz and gypsum with lesser components of clay minerals (illite and kaolinite), albite, and muscovite/(sericite) (Table 1).

Oriented specimens were prepared from each sample to further investigate the clay mineralogy. The XRD spectra (Fig. 7) show strong mineral homogeneity and the presence of two mineral types (Table 1): (1) minerals of hydrothermal origin, represented predominantly by clays (illite and kaolinite), jarosite, and gypsum and (2) minerals originated from the granitic rocks including quartz, albite, and muscovite.

A detailed SEM investigation focused on the secondary products from the infill material was performed with EDS analyses to (semi)quantitatively determine the composition of the investigated phases. These main secondary phases include clay minerals, represented by illite $(K,H_3O)(Al,Mg,Fe)_2(Si,Al)_4O_{10}[(OH)_2,(H_2O)]$ and kaolinite $Al_2Si_2O_5(OH)_4$, and sulphate minerals, represented by jarosite $KFe^{3+}{}_3(SO_4)_2(OH)_6$ and gypsum $CaSO_4{\cdot}2H_2O$.

Kaolinite was identified in most of the analyzed samples and frequently associated with illite. The SEM images show typical fine-sheeted tabular crystals of approximately hexagonal shape and less than 5 µm in size (Plate III, a, b). The EDS spectra collected from samples 795-2 (Plate III, b) and 796-1 (semi)quantitatively indicate the presence of oxygen (58.9–63.6 wt.%), silicon (19.0–21.78 wt.%), and aluminum (14.5–17.7 wt.%) as the main kaolinite components, in addition to lesser amounts of iron (0.4–1.4 wt.%) and potassium (0.3–1.5 wt.%), most likely from the associated iron hydroxides and illite, respectively.

Illite is present in all of the analyzed samples and the SEM images reveal a typical sponge-like arrangement of fine fibrous crystals (Plate III, c). The EDS spectra collected on the illite crystals from

samples 794-7 and 795-2 (semi)quantitatively indicate the presence of oxygen (50.4–63.6 wt.%), silicon (5.3–19.2 wt.%), aluminum (3.2–14.8 wt.%), and potassium (1.3–2.4 wt.%) as the main components and lesser amounts of iron (0–0.7 wt.%), sulfur (0–4.0 wt.%), and phosphorous (0–1.2 wt.%).

Gypsum is present as tabular crystals up to 25 μm in length (Plate III, d). The EDS spectra indicate the presence of calcium (13.5 wt.%), sulfur (11.5 wt.%), and oxygen (50.3 wt.%) as the main chemical components.

Jarosite is present as isometric rhombohedral crystals (<2 μm) and frequently associated with clay minerals (Plate IV, a–d). The EDS spectra collected from three crystals indicate that the main components of jarosite are as follows: O = 48.4–59.2 wt.%; Fe = 19.9–38.3 wt.%; S = 4.7–8.6 wt.%; K = 1.0–1.1 wt.%; Na = 0.6–0.7 wt.%; and P = 1.2–1.3 wt.%.

Discussion

The granitic rocks of the Bozgai quarry underwent degradation processes owing to andesite-related hydrothermal activity and exposure to atmospheric oxygen and meteoric water, especially in the upper part of the magmatic body. Weathering processes led to the chemical/mineralogical and physical degradation of the rocks in the formation of secondary phase assemblages. Subsequential physical degradation occurred, which contributed to the rock disaggregation, significantly influenced the slope stability, and ultimately led to the formation of a debris cone. A spatial zonation of weathering processes is observed, with the highest-intensity alteration located at the granite-andesite contact and decreasing intensity with increasing distance from the contact.

Joints, fractures, and micro-fractures are widely accepted to exert a significant influence on granite weathering (e.g., Hill 1996). Veins up to few millimeters in thickness are present in the studied rocks and infilled with minerals that precipitated from andesite-related hydrothermal solutions consisting of quartz, calcite, pyrite, marcasite, and clay minerals. Hydrothermal solutions also affected the most sensitive minerals from the granitic and andesitic rocks (e.g., feldspars, mafic minerals) and common secondary phases formed, including clay minerals, chlorite, sericite, and iron hydroxides. The secondary phases precipitated on the surface of the primary minerals but mostly as infill material along the discontinuities of the granitic rock. The secondary minerals are visible with the naked eye owing to their white-yellowish color and occasional rusty pigments of iron hydroxides, as well as their characteristic fine crystals or granular masses developed as films on the exposed wall of the discontinuities.

The investigated infill material contains common secondary phases, such as kaolinite, illite, sericite, and iron hydroxides that developed on the primary minerals of the granitic and andesitic rocks. Kaolinite and illite are common secondary minerals that form via feldspar alteration.

As summarized by Hill (1996), there are three main opinions in the literature regarding the source of granite weathering: (1) solely by meteoric waters; (2) hydrothermal fluids; and (3) initial hydrothermal alteration or "pre-conditioning" followed by supergene alteration. Taking into account the spatial relationship of the secondary parageneses with hydrothermal veins, as well as the observed weathering zonation, the hydrothermal alteration in the studied quarry was likely followed by supergene alteration, as proposed by Dixon and Young (1981) and Young and Dixon (1983).

The presence of supergene alteration is supported by the presence of jarosite, which results from the alteration of iron sulfides (pyrite and marcasite) from the hydrothermal veins in the presence of meteoric water and atmospheric oxygen. Jarosite is a well-known secondary sulphate that precipitates in acidic environments in connection with sulfide mineral oxidation, including acid rock and acid mine drainages (Hochella et al. 2005; Forray et al. 2010). Iron sulfides such as pyrite and marcasite of hydrothermal origin observed in the hydrothermal veins are the source for iron and acidity. In the presence of meteoric water and atmospheric oxygen, the iron sulfides transformed and sulfuric acid was released as follows (Har et al. 2019):

$$2FeS_2 + 7O_2 + 2H_2O \rightarrow 2\,Fe^{2+}SO_4 + 2H_2SO_4$$

The oxidation of pyrite/marcasite also occurred:

$$FeS_2 + O_2 + 2H_2O \rightarrow Fe^{2+} + 2\,SO_2^{2-} + 4H^+$$

The Fe^{2+} produced through this reaction could then react with O_2 to form Fe^{3+} (McGregor et al. 1998; Nordstrom 1982):

$$4Fe^{2+} + O_2 + 4H^+ \rightarrow Fe^{3+} + 2H_2O$$

Another possible reaction path for the precipitation of Fe^{3+}-bearing phases is the formation of amorphous ferric hydroxide, which can explain the rusty color of the secondary products:

$$Fe^{3+} + 3H_2O \rightarrow Fe(OH)_3 + 3H^+$$

The jarosite mineral group is defined by the general formula $AFe_3(SO_4)_2(OH)_6$ where A sites are commonly occupied by alkali ions such as K^+ (potassium jarosite) or Na^+ (natrium jarosite) or $(H_3O)^+$ (hydronian jarosite). Granitic K-feldspar represents an important K^+ source and jarosite forms by the following reaction (McGregor et al. 1998):

$$K^+ + 3\ Fe^{3+} + 2\ SO_2^{2-} + 6\ H_2O \rightarrow K\ Fe_3(SO_4)_2(OH)_6$$

The EDS spectra collected from the jarosite crystals in this study also indicate the presence of Na^+, which also fits well with the geochemistry of the weathering environment where Na^+ can originate from the granitic plagioclase feldspars that undergo hydrothermal alteration.

The reaction between secondary calcite ($CaCO_3$) of hydrothermal origin and H_2SO_4 generated in an acidic environment in the presence of water can lead to the formation of gypsum:

$$CaCO_3 + H_2SO_4 + H_2O \rightarrow CaSO_4{\cdot}2H_2O + CO_2$$

Gypsum is a main component of the infill material but the X-ray peak intensities are lower in the oriented samples (e.g., the maximum registered counts at $2\Theta = 11.59°$ is 2000 in the oriented samples but up to 6400 in the natural samples). This decrease of peak intensity is likely the result of gypsum dissolution in the suspension water during preparation of the oriented samples.

Gypsum solubility is also possible in the natural environment. In the presence of meteoric water, gypsum dissolution can occur (up to 2.0 g/L) to form an unsaturated state solution depending on particle size. Previous experimental studies have shown that the maximum gypsum dissolution occurs for particle sizes less than 1 μm (Lebedev and Kosorukov 2017).

Conclusions

The granitic body pierced by an andesitic dyke in the Bozgai quarry represents a precarious situation in terms of rock slope stability. In a natural environment, such as a quarry that has been inactive for more than 40 years, degradation processes under the influence of meteoric water and atmospheric oxygen lead to the disaggregation of granitic rock and the formation of debris cones.

Andesite-related hydrothermal activity affected both the andesitic and granitic rocks and consequently led to the formation of secondary minerals represented by clay minerals (kaolinite and illite), pyrite, marcasite, sericite, and iron hydroxides. The secondary minerals developed on the

primary minerals or were deposited as infill material in the veins of a few millimeters in thickness, crossing both the andesite and granite.

The exposure of this particular material to atmospheric weathering over many years created the ideal conditions for initiating a new alteration processes in a wet and oxidizing environment. The oxidization of pyrite and marcasite generated an acidic environment and sulphate minerals (e.g., jarosite, gypsum) precipitated. The formation of amorphous ferric hydroxide also took place in an oxidizing environment.

As a result of the two alteration stages, the final mineral assemblages consist of typical secondary phases including kaolinite, illite, sericite, gypsum, jarosite, and iron hydroxides accompanied by quartz, albite, and microcline. The presence of pyrite and marcasite influences the quality of extracted aggregates (Har et al. 2019) but also leads to formation of jarosite and gypsum. Rock slope stability is thus influenced by the alteration processes together with the structural characteristics of clay minerals and geochemical behavior of sulfates in the presence of water.

The abundance of kaolinite with its sheeted structure and possible sulphate dissolution in the presence of meteoric water favor the slipping of altered rock fragments and reduce rock slope stability. The identification of hydrothermal activity or any type of sulfides, especially iron sulfides (pyrite and marcasite), is thus crucial for rock slope stability predictions, as well as regarding the quality of raw materials used for concrete and asphalt aggregates.

Acknowledgments: We thank Esther Posner, PhD, from Liwen Bianji, Edanz Editing China (www.liwenbianji.cn/ac), for editing the English text of a draft of this manuscript.

Declarations

Funding:

This study was financially supported by Babeş-Bolyai University of Cluj-Napoca through research contract no. 35525/26.11.2019, internal competition “Special scholarships for scientific activities for students based on the research projects and dissemination of the results”.

We confirm that there are no known conflicts of interest associated with this publication. We confirm that the manuscript has been read and approved by all named authors and that there are no other persons who satisfy the criteria for authorship but are not listed. We further confirm that the order of authors listed in the manuscript has been approved by all authors.

We confirm that we have given due consideration to the protection of intellectual property associated with this work and that there are no impediments to publication, including the timing of publication,

with respect to intellectual property. We confirm that we have followed the regulations of our institutions concerning intellectual property.

We understand that the corresponding author (Nicolae Har, nicolae.har@ubbcluj.ro) is the sole contact for the editorial process, including communication with the editorial manager and office. He is responsible for communicating with the other author regarding progress, revision submissions, and approval of the final proofs. We confirm that we have provided a current and correct email address for the corresponding author.

Cluj-Napoca: 16 March 2021

Conflicts of interest:

The authors declare that they have no known competing financial interests or personal relationships that could have appeared to influence the work reported in this paper.

Availability of data and material:

Not applicable

Code availability:

Not applicable

References

Anton DC (1999) Petrographical, geochemical and isotopic study of Mt. Mare Granitoids, North Apuseni Mountains - Evolution of paraluminous magma. Dissertation, University of Tokyo.

Balintoni I, Balica C, Cliveti M, Li-qiu Li, Hann H-P, Chen F, Schuller V (2009) The emplacement age of the Muntele Mare Variscan granite (Apuseni Mountains, Romania). Geol Carpath 60:495-504.

Braga S, Paquet H, Begonha A (2002). Weathering of granites in a temperate climate (NW Portugal): granitic saprolites and arenization. Catena, 49(1):41–56.

Bustin RM, Matthews WH (1979). Selective weathering of granitic clasts. Canadian Journal of Earth Science, 16, 216-223.

Cravotta III CA (1994). Secondary iron-sulfate minerals as sources of sulfate and acidity. C.N. Alpers, D.W. Blowes (Eds.), Environmental Geochemistry of Sulfide Oxidation, Am. Chem. Soc. Symp. Ser., vol. 550, 345-364.

Dimitrescu R (1966). Muntele Mare. A geologic and petrographic study. *An. Com. Geol.* 35, 165—239 (in Romanian).

Dixon JE, Young RW (1981) Character and origin of deep arenaceous weathering mantles on the Bega Batholith, southeastern Australia. Catena 8:97-109.

Forray FL, Smith AML, Drouet C, Navrotsky A, Wright K, Hudson-Edwards KA, Dubbin WE (2010) Synthesis, characterization and thermochemistry of a Pb-jarosite. Geochim Cosmochim Ac 74:215-224.

Hammarstrom JM, Seal II RR, Ouimette AP, Foster SA (2001). Sources of metals and acidity at the Elizabeth and Ely mines, Vermont: geochemistry and mineralogy of solid minewaste and the role of secondary minerals in metal recycling. In:Hammarstrom, J.M., Seal II, R.R. (Eds.), Environmental Geochemistry and Mining History of Massive Sulfide Deposits in the Vermont Copper Belt, Soc. Econ. Geol. Field Trip Guidebook Ser., vol. 35, II, 213–248.

Har N, Lăzărean A, Iliescu M, Ciont N, Abrudan IF (2019) Degradation processes of iron-sulfides and calcite containing aggregates from asphaltic mixtures. Constr Build Mater 212:745-754.

Hill SM (1996) The differential weathering of granitic rocks in Victoria, Australia. AGSO J Aust Geol Geophys 16:271-276.

Hochella J, Michael F, Moore JN, Putnis CV, Putnis A, Kasama T, Eberl DD (2005) Direct observation of heavy metal–mineral association from the Clark Fork River Superfund Complex: Implications for metal transport and bioavailability. Geochim Cosmochim Ac 69:1651-1663.

Kirschbaum A, Martínez E, Pettinari G, Herrero S (2005) Weathering profiles in granites, Sierra Norte (Córdoba, Argentina). J South Am Earth Sci 19:479–493

Lebedev AL, Kosorukov VL (2017) Gypsum solubility in water at 25°C. Geochem Inter 55: 205-210.

Lee SY, Kim SJ & Baik MH (2008) Chemical weathering of granite under acid rainfall environment, Korea. *Environ Geol* **55,** 853–862.

McGregor RG, Blowes DW, Jambor JL, Robertson WD (1998) Mobilization and attenuation of heavy metals within a nickel mine tailings impoundment near Sudbury, Ontario, Canada. Environ Geol 36:305-319.

Meunier A, Velde B (1982) Phengitization, sericitization and potassium-beidellite in a hydrothermally altered granite. Clay Minerals, 17(3):285–299.

Nordstrom DK (1982) Aqueous pyrite oxidation and the consequent formation of secondary minerals. In: Acid sulfate weathering. Soil Sci Soc Am, Madison, pp 37–56

Oberhardt N (2013) Granite weathering, saprolitization and the formation of secondary clay particles, SW Bornholm. *Master Thesis,* Department of Geosciences, Faculty of Mathematics and Natural Sciences, University of Oslo, 1-139.

Pană D (1998) Petrogenesis and tectonics of the basement rocks of the Apuseni Mountains. Significance for the Alpine tectonics of the Carpathian-Pannonian region. *Ph.D. Thesis*, *Univ. Alberta*, Canada, 1—356.

Săndulescu M (1984): Geotectonics of Romania. *Ed. Tehnica*, Bucuresti, 1—336 (in Romanian).

Ştefan A, Lazăr C, Berbeleac I, Udubaşa G (1988) Evolution of banatitic magmatism in the Apuseni Mountains and associated metallogenesis. DS Inst Geol 72-73:195-213.

Wilson MJ (2004) Weathering of the primary rock-forming minerals: processes, products and rates. Clay Miner 39:233–266.

Whitney DL, Evans BW (2010) Abbreviations for names of rock-forming minerals. Am Mineral 95:185-187.

Wyllie DC, Mah CW (2004) Rock slope engineering: Civil and mining, 4th edn. Spon Press: London.

Young RW, Dixon JE (1983) Weathering and hydrothermal alteration: Critique of Ollier's argument. Catena 10:439-440.

Figures

Figure 1

Typical set of tectonic discontinuities in granite of the Bozgai quarry. The image was taken from the second bench of the quarry where fresh microgranular granite is exposed

Figure 2

Spatial relationship between the host granitic rock and andesitic intrusion with the weathering zonation and debris cone on the slope on the 6th bench of the Bozgai quarry

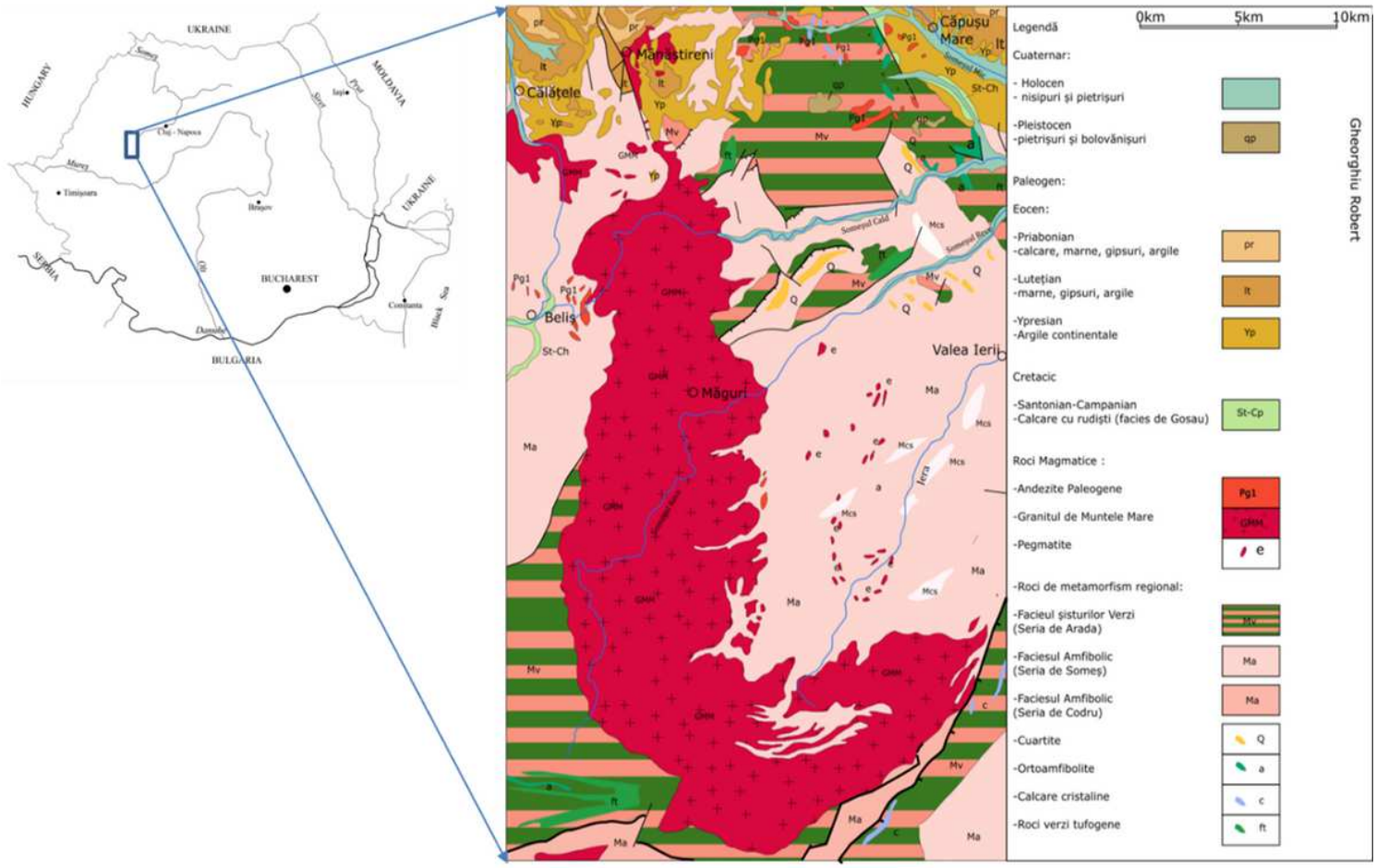

Figure 3

Geological map of the Muntele Mare granite massif outcrop area and location on a broader geographical map (based on 1:200,000 Romanian geological maps, Cluj and Turda sheets) Note: The designations employed and the presentation of the material on this map do not imply the expression of any opinion whatsoever on the part of Research Square concerning the legal status of any country, territory, city or area or of its authorities, or concerning the delimitation of its frontiers or boundaries. This map has been provided by the authors.

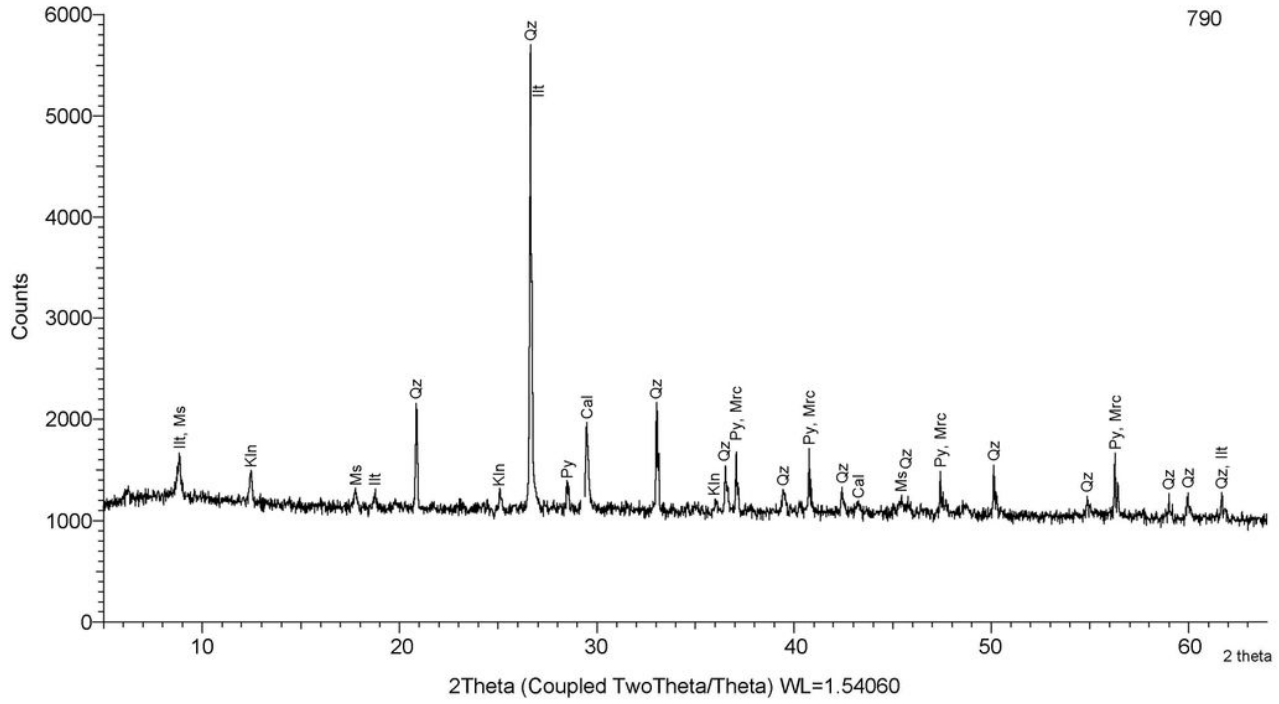

Figure 4

X-ray diffraction pattern of the infill material from sample 790 with specific peaks for quartz (Qz), calcite (Cal), pyrite (Py), marcasite (Mrc), illite (Ilt), kaolinite (Kln), and muscovite/sericite (Ms)

Figure 5

White-yellowish or rusty secondary minerals precipitated on the walls of the granite discontinuities

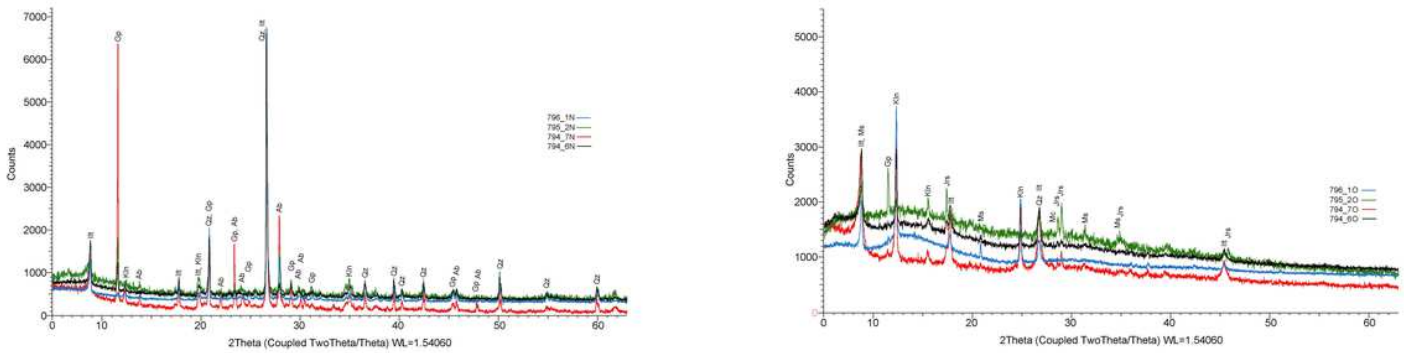

Figure 6

X-ray diffraction pattern of unoriented samples (794-6N, 794-7N, 795-2N, and 796-1N) collected from the infill material with specific peaks for quartz (Qz), illite (Ilt), gypsum (Gp), kaolinite (Kln), and albite (Ab)

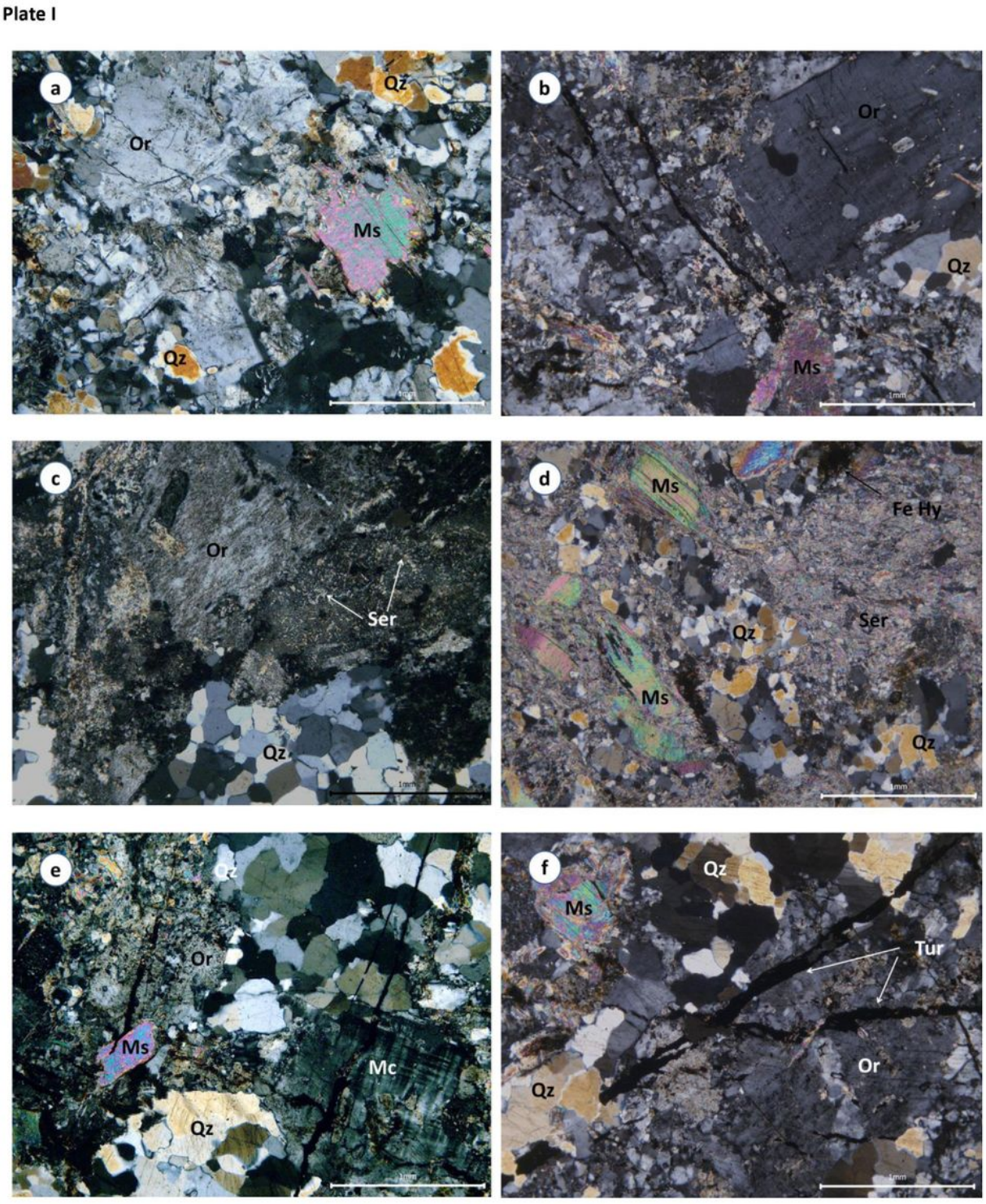

Figure 7

Plate I. Cross-polarized microscopic images show the mineralogical and petrographic aspects of the granite from the Bozgai quarry. a) Orthoclase (Or), quartz (Qz), and muscovite (Ms) in relatively fresh holocrystalline equigranular microgranite. b) Phenocrysts of orthoclase (Or) in a fine groundmass

consisting of feldspars, quartz, and muscovite in relatively fresh porphyritic granite. c) Altered granite showing quartz (Qz) and very fine secondary clay minerals (dusty aspect) and sericite (Ser) as the result of feldspar (orthoclase) hydrothermal alteration. d) Altered granite showing muscovite (Ms), quartz (Qz), iron hydroxides (Fe-Hy), and the very fine lamellae of sericite (Ser) replacing feldspar. e) Quartz (Qz), microcline (Mc), muscovite (Ms), and orthoclase (Or) partly transformed into clay minerals and sericite. f) Veins of tourmaline (Tur) in granite consisting of orthoclase (Or) partly transformed into clay minerals, quartz (Qz), and muscovite (Ms). Mineral abbreviations are according to Whitney and Evans (2010)

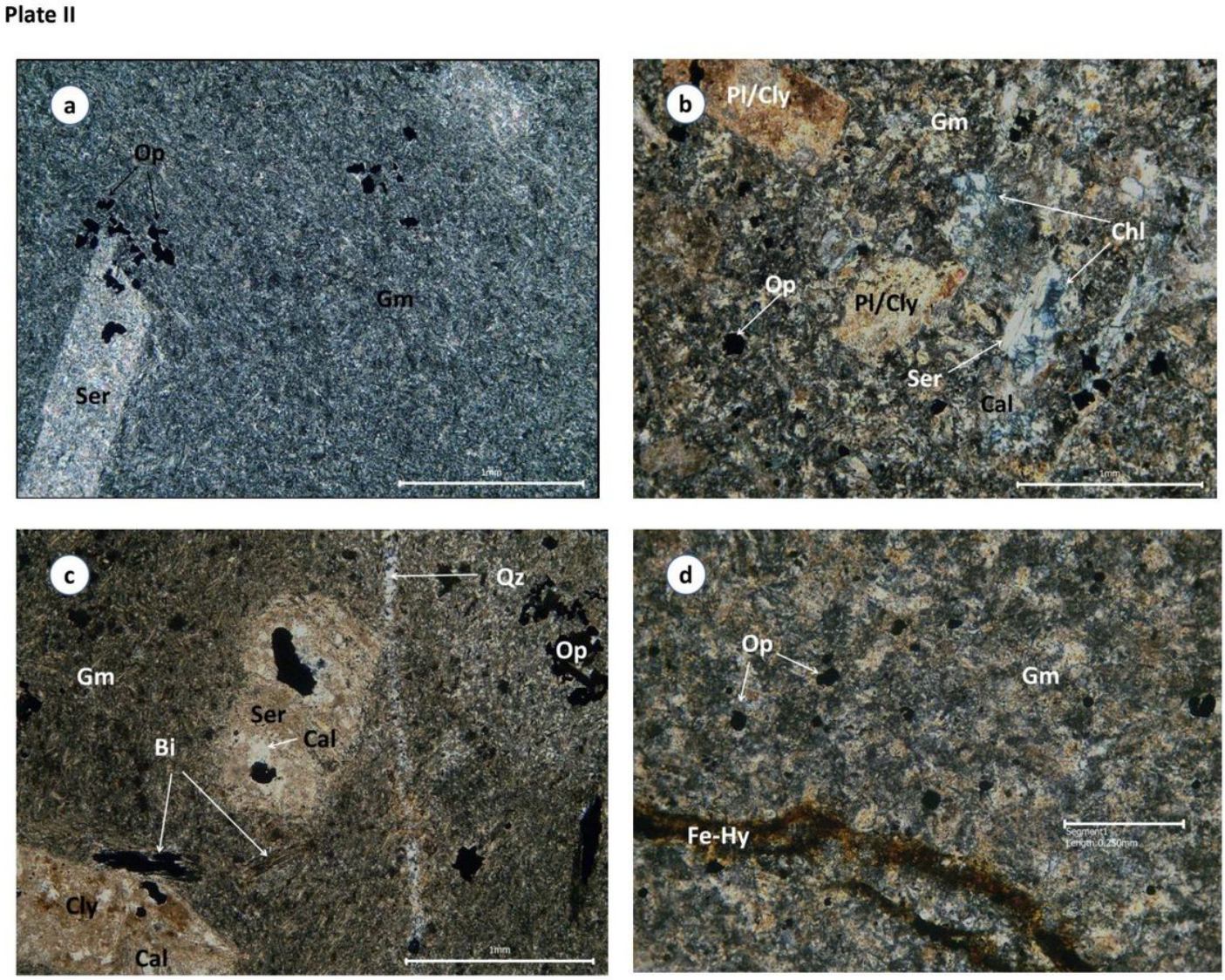

Figure 8

Plate II. Cross-polarized microscopic images show the mineralogical and petrographic aspects of the porphyritic andesite from the Bozgai quarry. a) Porphyritic texture of the andesite with a plagioclase phenocryst replaced by sericite (Ser) in a very fine groundmass (Gm) consisting of twinned plagioclase feldspars, opaque minerals (Op), and other secondary minerals. b) Former plagioclase feldspar phenocrysts replaced by clay minerals (Pl/Cy) in a groundmass (Gm) of opaque minerals (Op) and

secondary minerals represented by calcite (Cal), sericite (Ser), and chlorite (Chl). c) Former plagioclase phenocrysts replaced by clay minerals (Cy), sericite (Ser), and calcite (Cal), and former biotite (Bi) substituted by sericite and opaque minerals in a fine groundmass (Gm) with quartz-infilled veins. d) Detailed image of the iron-hydroxide (Fe-Hy) infilled veins in the groundmass (Gm) of altered andesite. Mineral abbreviations are according to Whitney and Evans (2010)

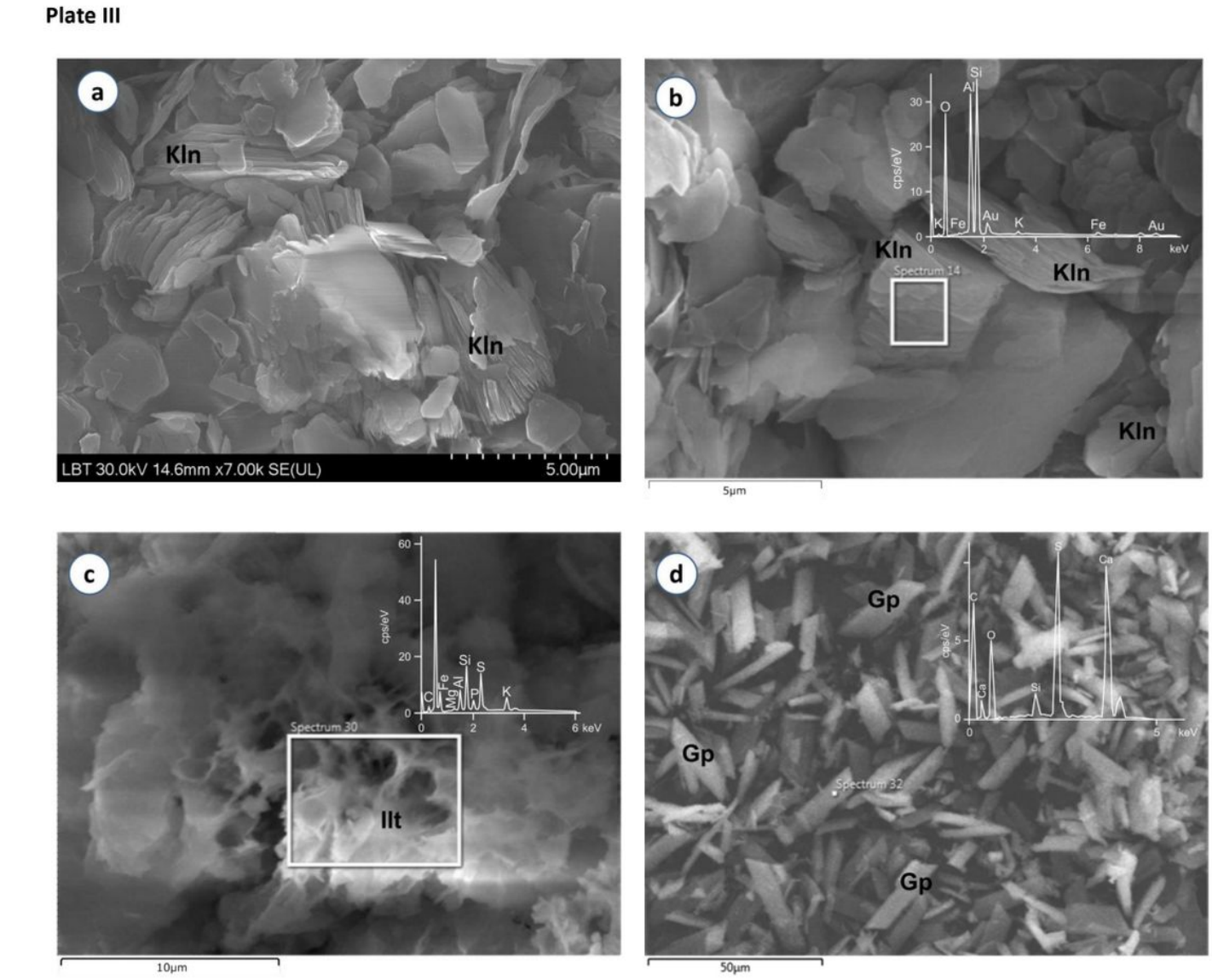

Figure 9

Plate III. SEM images and EDS spectra of infill material from the granite discontinuities represented by a, b) sheeted tabular kaolinite (Kln) crystals, c) sponge-like illite, and d) tabular gypsum crystals.

Plate IV

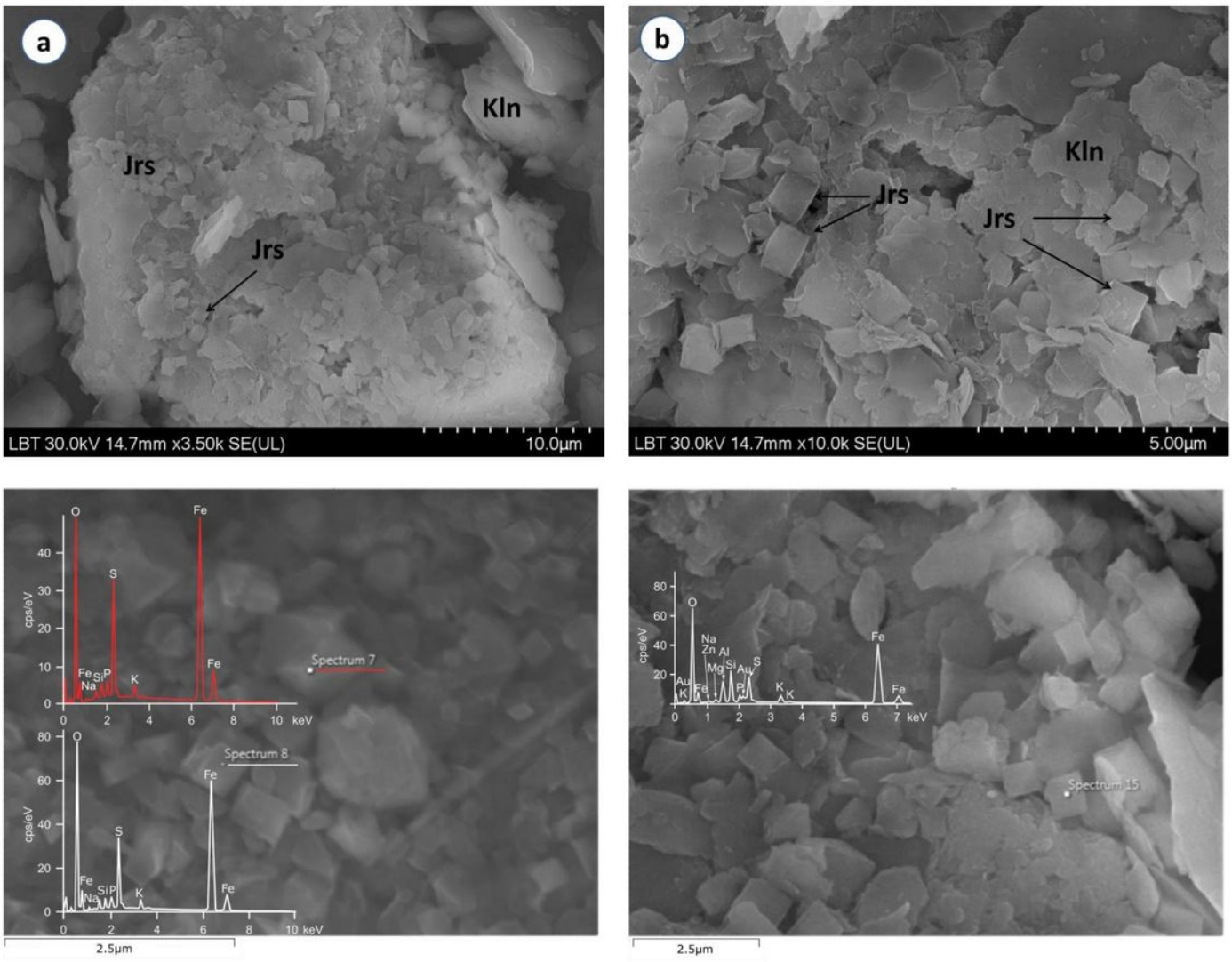

Figure 10

Plate IV. a–d) SEM images and EDS spectra of rhombohedral jarosite (Jrs) crystals associated with kaolinite (Kln) from the infill material of sample 795-2.